# An Orifice Flow Analysis on the Basis of Density and Viscosity Effects of Fluids

SANTOSH KUMAR PANDA
Mechnical Engineering Department,
NIST Institute of Science and Technology,
Berhampur, Odisha, PIN- 761008,
INDIA

*Abstract:* - The orifice flow measurement produces errors due to highly turbulent and backflow in downstream which have to be overcome. Determine the Δp, and coefficient of discharge ($C_d$) for flow through the orifice CFD analysis. The input parameters vary with the variance of Reynolds number (*Re*), fluids with the deviation of density and viscosity, area ratio ($\sigma$). The range of *Re* (20000- 100000), $\sigma$ (0.2- 0.6), density ($\rho_r$), and viscosity ($\mu_r$) ratio vary as per the fluids considered. The various incompressible and compressible fluids are considered for the study of flow through the orifice based on the difference in density and viscosity properties. The fluids considered for studies are Air, Ammonia ($NH_3$), Carbon dioxide ($CO_2$), Hydrogen ($H_2$), and Sulphur dioxide ($SO_2$) as compressible fluid category, and water ($H_2O$), liquid ammonia ($LNH_3$), liquid hydrogen ($LH_2$), liquid oxygen ($LO_2$), liquid *R12* (Dichlorodifluoromethane) as incompressible fluid category. Correlations are also proposed from the above numerical database to determine $C_d$ as a function of *Re*, $\sigma$, $\rho_r$, and $\mu_r$ for the orifice. The correlation provides a significant contribution to the viscous fluid flow measurement with the flow through the orifice.

*Key-Words:* - Area ratio, Coefficient of discharge, Multi-fluid, Orifice, Pressure drop, Viscosity.

Received: April 12, 2023. Revised: September 18, 2023. Accepted: November 14, 2023. Published: December 31, 2023.

## 1 Introduction

Orifice flow meter is a popular flow measuring equipment used for fluid flow measurement for a wider range of applications. The repeatability of measuring, dependability for a longer duration, a wider range of flow limit, and simplicity of design make the orifice more adaptable. In comparison to the flow meter such as the nozzle and venturimeters orifice gives better $\Delta p$ to determine the $C_d$. Bernoulli's principle is used to determine the fluid energy along the flow through the orifice. Two pressure taps are placed (one *2D* upstream and the other *0.5D* distance downstream) to determine the $\Delta p$ with the help of pressure measuring devices. The $\Delta p$ of the flow changes because of the vena-contractor (smallest cross-sectional area) of the orifice. A literature-based study reported on flow through an orifice to know the fundamental of the orifice, [1]. *Re* and $\sigma$ play an important role in the prediction of $\Delta p$ and $C_d$ based on correlation for different geometrical profile of the orifice. A perforated plate orifice is used to develop correlation, which is the function of *Re* and $\sigma$ for the prediction of $\Delta p$ and $C_d$, [2], [3]. Square-edged and concentric orifices used to develop correlation as a function of plate thickness, $\sigma$ and *Re*, [4]. The pressure loss coefficient for a circular orifice is determined based on a correlation, function of *Re*, $\sigma$, and reduction ratio, [5]. A comparison study for various profiles such as sloping-approach orifices, sharp-edged and streamlined orifices evaluated $\Delta p$ and energy loss in a flood conduit to minimize the cavitations effect, [6]. Discharge coefficient for orifices and nozzles are evaluated with equations to an orifice pipe flow, [7]. A series of correlations expanded for $\Delta p$ for a circular orifice on the variation of non-dimensional orifice number, thickness, and area ratio, [8]. Number of compressible natural fluids (air, $CO_2$, *Ar*, and *He*, and mixture of *Ar-He*) are considered as working fluids to determine $C_d$ for various flow devices such as orifice and nozzles, [9]. Air and water were considered for a numerical study for an orifice flow on the variation of Re, area, and space ratio to predicted $\Delta p$, [10]. Several fluids applied for orifice flow analysis for different fluids, [11], [12], [13], [14], [15], [16], for various applications of the flow through the orifice. High viscous fluids for small size orifices used such as molasses, [17], viscous fluids, [18], and high viscous fluids, [19], to determine the flow coefficient of an orifice flow. The orifice flow was used for a sharp-edge circular orifice with *R113* (Tri-chloro-tri-fluoro-methane) to develop several correlations for different fluid flows, [20], [21], [22]. Water-based flow analysis through the orifice considers for estimation of flow characteristics with variation of input parameters, [23], [24], [25], [26]. Multiple fluids are used in multi-phase analysis such as air-water, [27], [28], [29], [30], steam [31], wet gas [32], petroleum products [33], for the orifice flow to analyze two-phase studies.

Based on the literature study a flow analysis of an orifice to predict velocity profile, discharge coefficient ($C_d$), and pressure drop (*Δp)* for different compressible and incompressible fluids. Two no. of correlations will be estimated for the fluids (Compressible and Incompressible) flow through the orifice. The input parameters are varied such as Reynolds number (*Re*), area ratio ($\sigma$), and properties of fluids such as viscosity ($\mu_r$) and density ($\rho_r$) ratio to carry out the numerical studies.

# 2 Numerical Methodology

A geometrical model was prepared for the orifice with pipe flow for the numerical analysis of different fluids. Unstructured mesh is generated for the model with the use of *CFD* based software. The optimum solution to the numerical problem was achieved with the generation of high-class and aspect ratios for the grids. The mesh is discretized with a finite-volume method (*FVM*). Wall effects of the flow domain were improved by introducing more no grids to enable grid-independent studies. The circumference of the mesh volume improved by creating *O*-grid mesh size for uniform volumetric elements. Figure 1 presents a line sketch of the orifice model for the present studies. The dimension of the orifice is represented with nomenclature presented the Figure 1. The '*D*' is the diameter of the pipe, '*d*' is the diameter of the orifice, and '*l*' is the thickness of the orifice. The Three different '*D*' sizes are considered as 50.8 to 101.6 mm. The '*d*' dimensions are selected to maintain the *σ.* Figure 2(a) depicts the orifice province mesh structure and mesh volume of the orifice province. The Figure 2(b) is a enlarge view of two different orifice mesh geometries near the orifice zone shown for the present analysis.

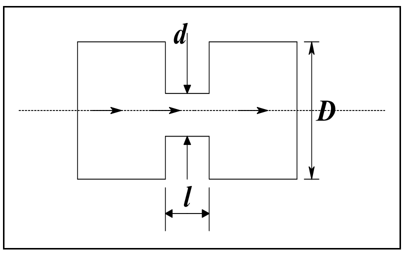


Fig. 1: Line sketch of the orifice model

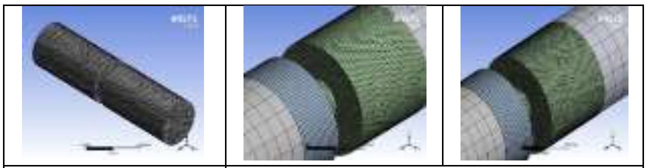

(a) Mesh topology

(b) Enlarge the view of the surface mesh in the orifice region with two different grid size

Fig. 2: Geometry and computational mesh of a present flow model

The fluids of compressible and incompressible flow are considered for the numerical study based on density and viscosity properties. The fluids are taken into account based on categories of property that differ from the based fluids. The base fluids for compressible flow are air and water for incompressible fluids. The fluids chosen for incompressible fluids are $LH_2O$, $O_2$, $LH_2$, *R12,* and $LNH_3$ as per the fluid property. Similar to compressible fluids are air, $NH_3$ gas, $CO_2$, $H_2$ gas, and $SO_2$. The fluids and their properties are mentioned in Table 1.

Table 1. Property of the fluids

| **Name** | **$\rho$ (kg/m$^3$)** | **$\mu$ (kg/m-s)** | **Name** | **$\rho$ (kg/m$^3$)** | **$\mu$ x10$^{-5}$ (kg/m-s)** |
|---|---|---|---|---|---|
| **Incompressible** | | | **Compressible** | | |
| $H_2O$ | 998.2 | 0.001 | Air | 1.225 | 1.79 |
| $LO_2$ | 1142 | 0.0002 | $NH_3$ | 0.6894 | 1.02 |
| $LH_2$ | 70.85 | 1.33e-5 | $CO_2$ | 1.7878 | 1.70 |
| *R12* liquid | 1130 | 0.0002 | $H_2$ | 0.0819 | 0.841 |
| $NH_3$ liquid | 610 | 0.00015 | $SO_2$ | 2.77 | 1.20 |

## 2.1 Governing Equation

The assumptions considered for the study are steady flow, and Newtonian fluid with the neglected compressibility factor.

Continuity $\nabla . u = 0$ (2)

Momentum $u.\nabla u = -\nabla p + \mu \nabla^2 u + \rho . g$ (3)

K.E $\nabla.(uk) = \nabla . \left[ \mu + \left( \frac{\mu_t}{\sigma_k} \right) \nabla k \right] + P_k - \varepsilon$ (4)

Energy dissipation rate equation

$$u.\nabla \varepsilon = \nabla . \left[ \mu + \left( \frac{\mu_t}{\sigma_\varepsilon} \right) \nabla \varepsilon \right] + C_{\varepsilon 1} \frac{\varepsilon}{k} P_k - C_{\varepsilon 2} \frac{\varepsilon^2}{k} \tag{5}$$

P= production term, $\mu_t$= eddy viscosity and

$$\mu_t = C_\mu \frac{k}{\omega},\ C_\mu = 0.09, C_{\varepsilon 1} = 1.44, C_{\varepsilon 2} = 1.44, \sigma_k = 1, \sigma_\varepsilon = 1.3$$

## 2.2 Grid Independence Study

A suitable optimized grid size is required to get accurate results for a numerical problem. The grid independence test is the method to get the optimized grid size for a geometric model. The present study has considered five different models as per the $\sigma$ concern. The grid-independent study for a model is reported in Table 2. The model size is $\sigma$ = 0.36, pipe diameter ($D$) = 101.6 mm considered with $Re$ = 60000 for grid-independent study for different grids as reported in Table 2. The grid shapes make an $O$-grid type and the wall intensity increases by introducing more no grids for accurate results. The mesh intensity increases near the orifice section and upstream of the orifice along the flow. The mesh element size decreases from 0.008 to 0.002 by increasing the number of mesh sizes. The mesh sizes considered for the independent study are 65.2, 103.5, 147.7, 315.7,885 million, among these 147.7 million mesh sizes give better results for the $\Delta p$ as mentioned in Table 2. The % increase in the $\Delta p$ calculated based on the formula mentioned in eq. (6) The grids on the mesh increase nearly the orifice to get a better flow profile. The study found 147.7 million gives better results as reported in Table 2.

Table 2. Mesh Independence study

| Sl no | 1 | 2 | 3 | 4 | 5 |
|---|---|---|---|---|---|
| Mesh Size | 65249 | 103573 | 147710 | 315700 | 885033 |
| $\Delta p$ (kPa) | 3434.6 | 3591.2 | 3653.2 | 3655.4 | 3656 |
| % increase in Δp | --- | 4.55 | 1.69 | 0.06 | 0.01 |

$$\%\text{ increase in}\Delta p = \frac{\Delta p_{\text{new mesh}} - \Delta p_{\text{previous mesh}}}{\Delta p_{\text{previous mesh}}} \times 100 \quad (6)$$

## 2.3 Numerical Solution

The governing equations used for the present study are mass, momentums, turbulent kinetic energy, and dissipation rate of turbulent energy (standard $K$-$\varepsilon$ model) for the compressible and incompressible fluids. The governing equations are present in Eqs. (2)–(5). Steady-state simulation carried out with the gravitational force acting against gravity and pressure based solver used for the numerical studies. Velocity inlet and pressure outlet boundary conditions used for the inlet and outlet to the orifice, and no-slip condition are used for the wall to define the flow domain. The fluids were selected as per the numerical studies required. The turbulence intensity was selected with 5% at the inlet with fully developed flow by assuming hydraulic diameter. *SIMPLE* (Semi-implicit method for pressure linked equation) algorithm used pressure-velocity coupling. The grids are discretized with the least square cell method. Standard scheme for pressure terms, second order upwind scheme has been used for momentum and turbulent equation terms. The under-relaxation factor (*URF*) used for pressure is 0.3, momentum 0.4 – 0.7, turbulent equation 0.8. The residual scale is considered as required the converge criteria. The solution is initialized before the simulation starts and the output result is collected after convergence of the problem.

# 3 Result Analysis

The computational envisaged result evaluated with the existing analysis represented in (Roul and Das, 2012) of the flow-through orifice analysis for the validation of the study. The above literature considered $H_2O$ as a single phase fluid. The parameters considered in the above article are an orifice of 60 mm diameter, $\sigma$ = 0.54 for different $Re$ = 30000 to 200000 to determine $\Delta p$. Similar computational case studies were taken account for the validation of the present analysis. Upto 5% error was found in the present study on the prediction of $\Delta p$.

The static pressures (*St. Pr.*) for different fluids along the flow length of the orifice are shown in Fig. 3(a) compressible fluids and Figure 4(a) for incompressible fluids. The decreasing orders of the *St. Pt.* along the compressible fluids are $CO_2$, $NH_3$ gas, $H_2$ gas, Air, and $SO_2$. The graph concludes that $H_2$ has maximum *St. Pt.* compared to other fluids. From the incompressible fluid point of view $H_2O$ gives maximum *St. Pt.* because of the high $\rho_r$, $\mu_r$. The static $\Delta p$ along the flow path of the orifice for variation in $Re$ is shown in Figure 3(b) for compressible fluids and Figure 4(b) for incompressible fluids.

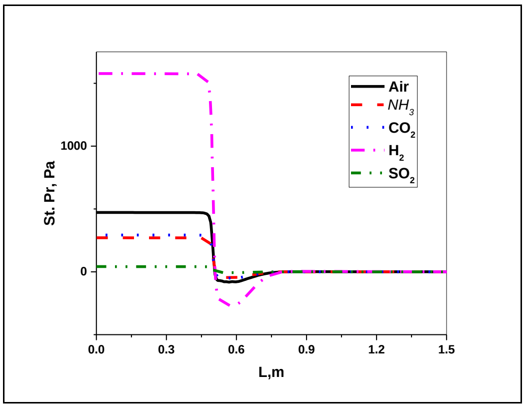


(a) Variation of fluids

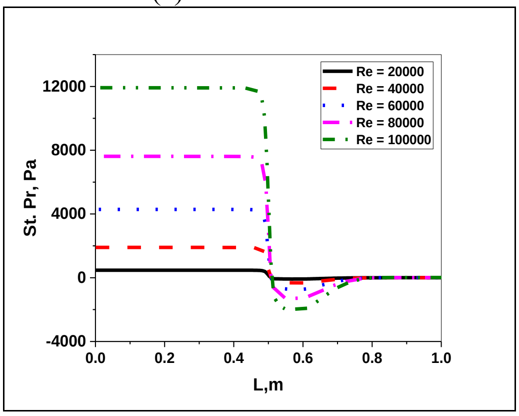


b) Variation with *Re* for air

Fig. 3: *St. Pr.* profiles for the compressible flow

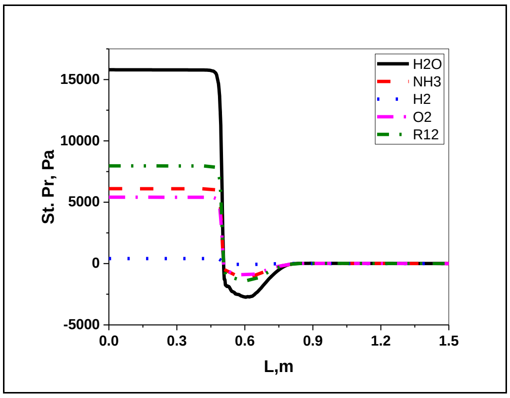


(a) Variation of fluids

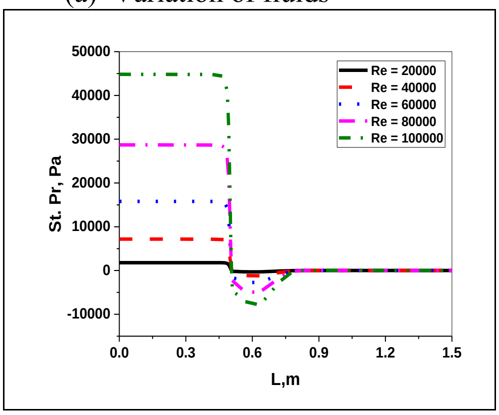


(b) Variation with *Re* for water

Fig. 4: *St. Pr.* profiles for the incompressible flow

Figure 5(a) and Figure 5 (b) demonstrate the *Δp* along the orifice flow for compressible and incompressible fluid on the variation of Re. The graphs found $H_2$ has maximum *Δp* for compressible fluids and $H_2O$ gives maximum *Δp* compared to the other incompressible fluids along the variation of *Re*. The $H_2$ has maximum because of better fluid properties compared to other fluids. The results were reported because of larger *St. Pr*. profile as mentioned in the above figures. The *Δp* increases as the *Re* increases because of an increase in the velocity of fluids because of a directly proportional relation.

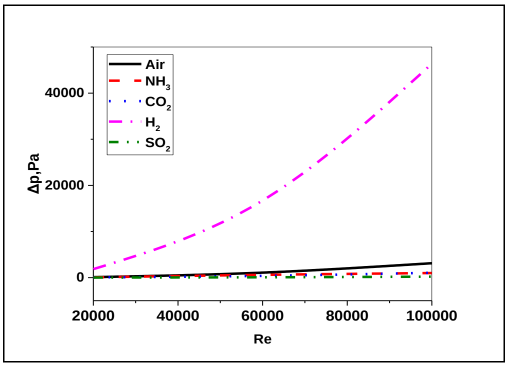


(a) Compressible flow

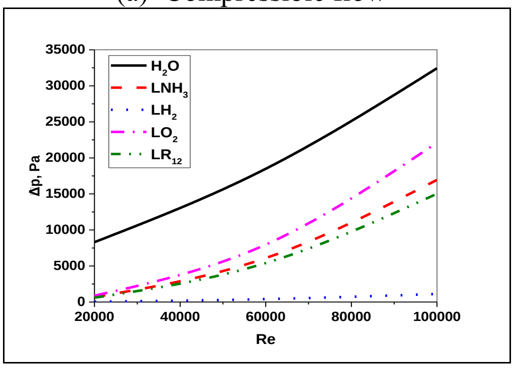


(b) Incompressible flow

Fig. 5: *Δp* on the variation of *Re*

The *Δp* varies with *Re* for different $\sigma$ as shown in Figure 6(a) and Figure 6(b) for compressible and incompressible fluids for an orifice flow. The smaller $\sigma$ founds more *Δp* for compressible and incompressible flows because of the narrow passage. The *Δp* decreases as the $\sigma$ value increases with a wider orifice area to the fluid flows. Figure 6 also found that the *Δp* is more for incompressible flow compared to compressible flow for a specified $\sigma$ value. Figure 7 reported the phenomena of $C_d$ for an orifice flow. The $C_d$ for compressible fluids shows that the values not vary much for different fluids as values vary from 0.56 to 0.67 for the variation of *Re* along the orifice flow. The $C_d$ values decrease as the *Re* increases as concluded because of smooth flow with the increase in the velocity of flow.

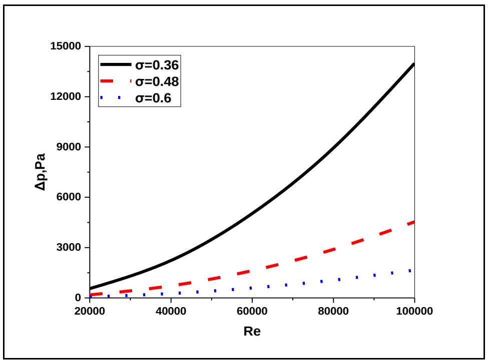


(a) Compressible flow

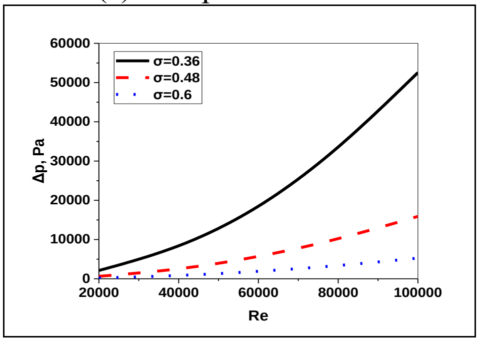


(b) Incompressible flow

Fig. 6: Δp on the variation of σ for orifice

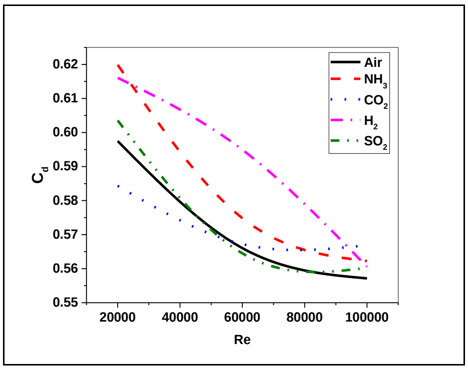


(a) Compressible flow

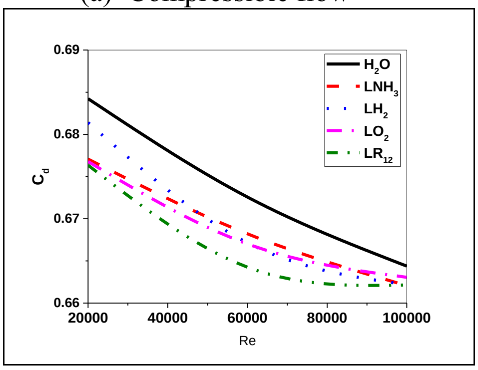


(b) Incompressible flow

Fig. 7: $C_d$ on the variation of *Re* for orifice

## 3.1 Correlation

Two correlations are proposed for $C_d$ for compressible and incompressible fluid along the orifice flow. The correlations are a function of *Re*, $\sigma$, and the non-dimensional parameters of density and viscosity. GARCH (Generalized Autoregressive Conditional Heteroskedasticity) is a MATLAB code that works on the principle of multi-regression tools to get coefficients of the correlations such as $C_1$, $C_2$, $C_3$, ..., etc. The correlation is represented in eq. (7-8) with correlation coefficient to be predicted. *GARCH* is a statistical tool used for the prediction financial outcome for a particular period from the present tendency which fits for the present numerical studies for developing the correlation. The correlation yields results with a 10% maximum margin of error. The correlation is as follows

$$C_d = f(Re, \sigma, \mu_r, \rho_r) \tag{7}$$

$$C_d = C_1.(\mathrm{Re})^{C_2}.(\sigma)^{C_3}.(\mu_r)^{C_4}.(\rho_r)^{C_5} \tag{8}$$

Where $\mathrm{Re} = \frac{\rho v d}{\mu}, \sigma = \frac{a}{A}, \mu_r = \frac{\mu}{\mu_b}, \rho_r = \frac{\rho}{\rho_r}$

The correlation functions $C_d$ = f ($Re, \sigma, \mu_r, \rho_r$) and correlation coefficient ($C_1$, $C_2$, $C_3$, $C_4$, $C_5$) for compressible and incompressible fluids are mentioned in Table 3. The correlation coefficient predicted the factorial relation between the input and output of the parameter for the analysis. The numerical result fits with the correlation data of an error within ±10% for both compressible and incompressible fluids. The error ±10% mentioned as a marginal trend line for the graphical presentation. The correlation is a function of *Re*, $\sigma$, and the property parameter $\mu_r$, $\rho_r$ which is a function of fluids. The range for the correlations is *Re* = 20000 to 100000, $\sigma$ = 0.3 to 0.6, $\mu_r$, and $\rho_r$ as the selection of the fluids.

Table 3. Correlation coefficients

| **Type of fluids** | $C_1$ | $C_2$ | $C_3$ | $C_4$ | $C_5$ |
|---|---|---|---|---|---|
| Compressible | 1.16 | 0.03325 | 0.43924 | 0.49007 | 0.38505 |
| Incompressible | 0.703 | 0.01195 | 0.0353 | -0.05691 | 0.07419 |

# 4 Conclusions

Numerical studies for an orifice were carried out to determine the velocity profile, Static pressure profile (*St. Pr.*), $C_d$, and $\Delta p$ for a fluid flow. The flow fluids are considered as per the compressibility and incompressibility nature based on the properties of density and viscosity. *Re* and $\sigma$ are the other input parameters for the study. The output parameters are compared with air for compressible flow and water for incompressible flow fluids. The study concludes that changing viscosity and density affects the $\Delta p$, $C_d$, and other flow profiles. The $C_d$ value predicts 0.56 to 0.67 which is particular for different applications of orifice flow. Based on the numerical prediction of the results two different correlations developed for compressible and incompressible fluids. The above study considers of different categories of fluids and properties such as the compressibility of fluids for further analysis. The correlations developed based on the $\mu_r$, *and* $\rho_r$ and predicted up to ±10% agreement for the numerical prediction database. The study will help to calibrate the mass flow measurement and controlling device for different fluids.

*References:*

[1] Panda S.K., Choudhury B. K., Rath K. C., (2022) A Literature Review on Orifice as a Flow Measuring Device, ECS Transactions, vol. 107(1), pp. 815. https://doi.org/10.1149/10701.0815ecst.

[2] Idelchik I. E., Malyavskaya, G. R., Martynenko, O. G., and Fried, E., (1994). Handbook of Hydraulic Resistances, *CRC Press*, Boca Raton.

[3] Gan G., Riffat S. B. (1997). Pressure loss characteristics of orifice and perforated plates, *Experimental Thermal and Fluid Science*, vol. 14, pp.160-165.

[4] Shanfang H., Taiyi M., Dong W., Zhong L. (2013). Study on the discharge coefficient of perforated orifices as a new kind of flowmeter, *Experimental Thermal, and Fluid Science*, vol. 46, pp. 74-83.

[5] Bullen P. R., Cheeseman, D. J., Hussain L. A., and Ruffel A. E., (1987). The Determination of Pipe Contraction Coefficients for Incompressible Turbulent Flow, *Int. J. Heat Fluid Flow*, vol. 8, pp. 111–118.

[6] Zhang Z. and Cai, J., (1999). Compromise Orifice Geometry to Minimize Pressure Drop, *Journal of Hydraulic Engineering*, vol. 125(11), pp. 1150-1153.

[7] Grace H. P., and Lapple C. E., (1951). Discharge Coefficient of Small Diameter Orifices and Flow Nozzles, *Trans. ASME*, 73, pp. 639–647.

[8] Panda S.K., Rath K.C., Choudhury B.K, (2023). Determining the flow correlation for an orifice with a non-dimensional number, *Flow Measurement, and Instrumentation*, vol. 90, pp. 102338.

[9] Kayser John C., Shambaugh Robert L. (1991). Discharge coefficients for compressible flow through small-diameter orifices and convergent nozzles, *Chemical Engineering Science,* vol. 46, No. 7, pp. 1697-1711.

[10] Panda S.K., Patra A. (2021). Determination of Coefficient of Contraction of Orifice with Variation of Geometrical Parameter. In: Palanisamy M., Ramalingam V., Sivalingam M. (eds) *Theoretical, Computational, and Experimental Solutions to Thermo-Fluid Systems*. Lecture Notes in Mechanical Engineering. Springer, Singapore.

[11] Johansen F. C., (1930). Flow through Pipe Orifices at Low Reynolds Numbers, *Proceedings of the Royal Society of London, Series A, Containing Papers of a Mathematical and Physical Character*, vol. 126(801), pp. 231-245.

[12] Tuve G. L. and Sprenkle R. E., (1933). Orifice Discharge Coefficients for Viscous Liquids, *Instruments*, vol. 6(1), pp 210-206.

[13] Kiljanski T., (1993). Discharge Coefficients of Free Jets from Orifices at Low Reynolds Numbers, *ASME Journal of Fluids Engineering*, vol. 115(4), pp. 778-781.

[14] Hasegawa T., Suganuma, M., and Watanabe, H., (1997). Anomaly of Excess Pressure Drops of the Flow through Very Small Orifices, *Physics of Fluids*, vol. 9(1), pp. 1-3.

[15] Samanta A. K., Banerjee T. K. and Das S. K. (1999), Pressure Losses in Orifices for the Flow of Gas-Non-Newtonian Liquids, *The Canadian Journal of Chemical Engineering*, vol. 77(3), pp 579-583.

[16] Valle D. D., Philippe A. T. and Carreau P. J. (2000). Characterizations of the Extensional Properties of Complex Fluids Using an Orifice Flowmeter, *Journal of Non-Newtonian Fluid Mechanics*, vol. 94(1), pp. 1-13.

[17] Dugdale D.S. (1997), Viscous flow through a sharp-edged orifice, *Int. J. Engg. Science*, vol. 35 (8), pp. 725-729.

[18] Mincks L. M. (2002), Pressure Drop Characteristics of Viscous Fluid Flow across Orifices, Mechanical Engineering, Iowa State University, Ames, *MS Thesis*.

[19] Bohra L. K., (2004). Flow, and pressure drop highly viscous fluids in small aperture orifices, Mechanical Engineering, Georgia Institute of Technology, *MS Thesis*.

[20] Kojasoy G., Kwame M. P., and Chang, C. T., (1997). Two-Phase Pressure Drop in Multiple Thick and Thin Orifices Plates, *Exp. Thermal Fluid Sci*., vol. 15, pp. 347–358.

[21] Lin Z. H. (1982). Two-Phase Flow Measurement with Sharp Edge Orifices, *Int. J. Multiphase Flow*, vol. 8, pp. 683–693.

[22] Singh G.M, Hrnjak P.S., Bullard C.W., (2001). Flow of refrigerant 134a through orifice tubes, *HVAC &R Research*, vol. 7 no. 3, pp. 245-262.

[23] McNeil D. A., Addlesee J. and Stuart A., (1999). An Experimental Study of Viscous Flows in Contraction, *Journal of Loss Prevention in the Process Industries*, vol. 12(4), pp. 249-258.

[24] Kim B. C., Pak, B. C., Cho, N. H., Chi, D. S., Choi, H. M., Choi, Y. M. and Park, K. A., (1997). Effects of Cavitation and Plate Thickness on Small Diameter Ratio Orifice Meters, *Flow Measurement and Instrumentation*, vol. 8(2), pp. 85-92.

[25] Ramamurthi K. and Nandakumar K., Characteristics of Flow through Small Sharp-Edged Cylindrical Orifices (1999). *Flow Measurement, and Instrumentation*, vol. 10(3), pp 133-143.

[26] Miller R. W. (1979). The Stolz and ASME-AGA Orifice Equations Compared to Laboratory Data, *ASME Journal of Fluids Engineering*, vol. 101(4), pp. 483-490.

[27] Alimonti C., Falcone G., Bello O. (2010)., Two-phase flow characteristics in multiple orifice valves, *Experimental Thermal and Fluid Science* vol. 34, pp. 1324–1333.

[28] Chisholm D., Flow of incompressible two-phase mixtures through sharped-edged orifices, *Mechanical Engineering Science* vol. 9, pp. 72–78 (1967).

[29] Fossa M., and Guglielmini G., Pressure Drop, and Void Fraction Profiles during Horizontal Flow through Thin and Thick Orifices, *Exp. Thermal Fluid Sci*., vol. 26, pp. 513–523 (2002).

[30] Roul M. K., Dash S., Single-Phase and Two-Phase Flow Through Thin and Thick Orifices in Horizontal Pipes, *Journal of Fluids Engineering, ASME*, vol. 134, pp. 091301-1(2012).

[31] Aguta R. M., Olsen K. E., Boe A., Saasen A., Aas B., Short communication Experimental investigation of liquid accumulation effects during orifice gas metering of two-phase flow, *The Chemical Engineering Journal* vol. 59, pp. 281-285 (1995).

[32] Geng Y., Zheng J., Shi T., Study on the metering characteristics of a slotted orifice for wet gas flow, *Flow Measurement, and Instrumentation,* vol. 17, pp. 123–128 (2006).

[33] Gassan H. Abdul-Majeed A., Maha R. A., Correlations developed to predict two-phase flow through wellhead chokes, *The Journal of Canadian Petroleum Technology* vol. 30, pp. 47–55 (1991).

**Contribution of Individual Authors to the Creation of a Scientific Article (Ghostwriting Policy)**

The author contributed in the present research, at all stages from the formulation of the problem to the final findings and solution.

**Sources of Funding for Research Presented in a Scientific Article or Scientific Article Itself**

No funding was received for conducting this study.

**Conflict of Interests**

There is no conflict of interest.